Design of an Exoskeleton Mechanism for the Shoulder Joint

Evangelos Papadopoulos, Georgios Patsianis
Department of Mechanical Engineering, National Technical University of Athens
Athens, Greece

Abstract - *This paper focuses on the design of a 2-DOF exoskeletal mechanism for the lateral and frontal abduction of the human upper limb. Major consideration was placed on the location of the center of rotation of the humerous with respect to the scapula. An experimental procedure for the determination of the kinematics of the shoulder girdle area using a CMM machine is described. The motion of the center of rotation of the shoulder is obtained using a Geneva mechanism. Kinematical analysis of the proposed hybrid mechanism is discussed and a validation study is presented. A 3D CAD model of the mechanism is presented and a FEM analysis illustrates the stability and durability of the portable mechanism. It is expected that the mechanism under development will help people suffering from muscle atrophy or to accelerate injured people recovery.*

Keywords: exoskeleton, intermittent mechanism, design.

I. Introduction

Progress in robotics and mechatronics, new lightweight and strong materials and more capable and efficient actuators give a new thrust to the proliferation of exoskeletons. Such devices are mechanisms designed to be mounted on a person's body, capable of following the person's motions and of applying forces or torques on him or her. In the non-technical area of applications, exoskeletons are becoming important in assisting elderly or physically weak people function without help, in treating people with chronic acute arm impairments, in rehabilitating people injured in accidents or in war, and in temporarily supporting people suffering from muscle atrophy. In the cases of muscle atrophy especially, such a device can be used together with physical therapy in order to accelerate the recovery process.

Among the human joints, the shoulder joint is an important one, as many human motions require its use. On the other hand, this joint is one of the most complex, and therefore the design of exoskeleton devices for the shoulder joint is quite involved. Many of the exoskeletons described in the literature are mechanisms designed with seven degrees of freedom (DOF). In most of these mechanisms, the glenohumeral joint is modeled as a 3-DOF ball and socket joint and therefore, it does not include translation of the glenohumeral joint and thus of the centers of rotation, [1]. There is also a number of passive exoskeletons (unactuated devices) such as the *MB Exoskeleton* developed for the U.S. Air Force [2], and wheel-chair mounted exoskeletons, such as the Motorized Upper Limb Orthotic System (*MULOS*), [3]. The basic characteristic of the later is that there is no compensation for the scapulothoracic motion, which is considered critical for shoulder rehabilitation. *MULOS* researchers examined the translation of the glenohumeral (GH) joint for several tasks, and deemed that the motion was not important in their application [4]. Some information on how the center of rotation of the shoulder joint is incorporated into the design of an exoskeleton, is provided by Kazuo Kiguchi and his associates in [5] – [12].

In this paper, the design of a mechanism for a robot arm exoskeleton for the lateral, see Fig. 1, and frontal abduction used for shoulder rehabilitation is examined. This mechanism aims to follow the human movement of the scapula and particularly the movement of the humerous with respect to the scapula. The hybrid mechanism developed employs a Geneva mechanism and a four-bar mechanism.

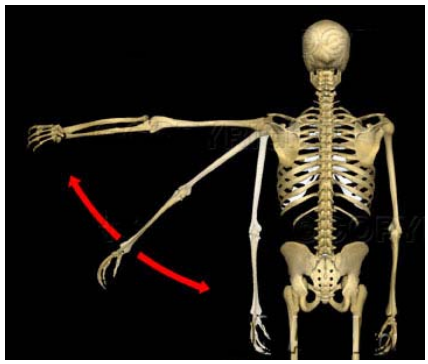

Fig 1. Lateral abduction and adduction of the upper arm from 0^o to 90^o.

A method for the determination of the shoulder kinematics is described. The method uses a Coordinate Measuring Machine (CMM) machine and yields a number of coordinates that describe the motion of the humerous head with respect to the scapula. To this end, a plastic humeral splint is used to provide the desired measuring points on the humerous. From the results obtained, the motion of the center of rotation (CR) of the GH joint was identified, and showed that during lateral abduction, two distinct CRs exist. Based on these results, the 2-DOF mechanism design has to allow lateral arm rotation from

email: egpapado@central.ntua.gr

0^o to 180^o and at the same time translate the CR to a new position for the second phase of abduction (50^o to 180^o). These requirements were achieved by a 4-slot Geneva mechanism in conjunction to a four-bar mechanism moving the CR of the humerous about 3 mm upwards in the glenoid fossa. The paper describes the kinematics of the mechanism, and presents evaluation results based on a Lego prototype. A Finite Element Analysis (FEA) of the mechanism CAD model shows that most of the device can be produced from epoxy resins minimizing the weight.

II. Determination of Shoulder Kinematics

The major thrust of this work is to design a portable, lightweight, accurate and energetically autonomous mechanism for the lateral and frontal abduction – adduction. To design the arm exoskeleton, and avoid mechanism-induced pain to a patient, it is essential to have kinematical data on the shoulder motion. Because of the limited available mechanical or kinematical data, an experiment to determine the motion of certain upper arm points was designed. To improve the accuracy of the measurements, a plastic humeral splint with holes on it was placed on subjects, Fig. 2a. These holes were used as measuring points representing the corresponding points on the human arm. To measure hole locations, a FARO Platinum arm portable CMM (FARO IND-01) with six dofs and workspace of 2.4 m, see Fig. 2b was used, [15].

(a) (b)

Fig. 2. (a) The plastic humerous splint with the holes on top of it (black dots), (b) Experimental setup consisting of the FARO IND-01 CMM arm placed on the right and the corresponding software for data acquisition.

Three groups of measurements were taken, each one at a different plane, starting from a plane parallel to the human back, followed by a plane at 45^o, and finally by one at 90^o. All measurements were made on a stretched arm moving upwards from 0^o (complete adduction) to 180^o (complete abduction) at 20^o to 25^o intervals, see Fig. 3. The experimental process carried out was simple and each measurement took about 2s. Both the measurement points and *joint coordinate system* (JCS) were chosen based on the guidelines of the *Standardization and Terminology Committee*, (STC), of the International Society of Biomechanics [13]. In Fig. 4 the anatomical bony landmarks and local coordinate system of the thorax are presented. The bony landmarks refer to:

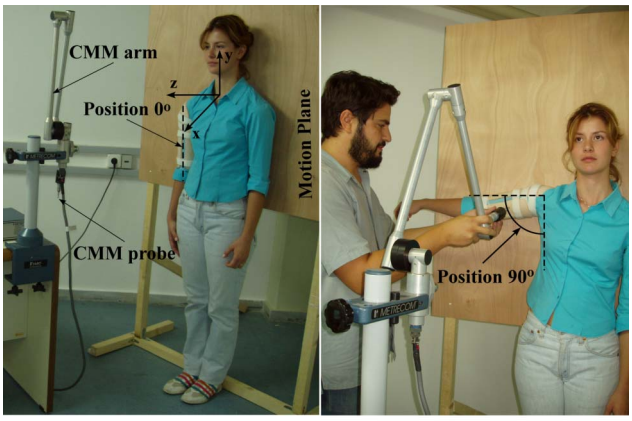

(a) (b)

Fig. 3. Experimental measurement procedure with the CMM. (a) The plane of motion, the resting point at 0^o and the components of CMM, (b) the arm rests in 90^o (half abduction).

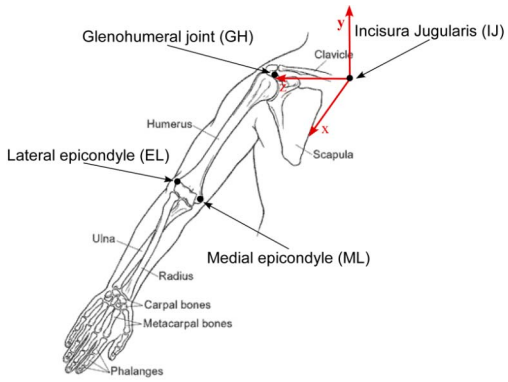

Fig. 4. Anatomical bony landmarks and local coordinate system based on the STC guidelines.

Thorax: IJ: Incisura Jugularis (suprasternal notch)
Humerous: GH: Glenohumeral rotation centre
EL: Caudal point on lateral epicondyle
EM: Caudal point on medial epicondyle

The results obtained contained the coordinates of the measured points for all positions and planes. The data was grouped and analyzed yielding a locus of points, representing the lateral abduction of the human right upper limb. In Fig. 5, the straight lines represent the clavicle and the humerous. It can be seen that the humerous head rotates about two distinct CR, proving that it moves upward in the glenoid fossa for approximately 3 mm. Therefore, it is concluded that the humerous motion must be divided in two parts. The first part corresponds to a purely rotational motion in which the arm moves from 0^o to 37^o, while the second part corresponds to a combined translational and rotational motion from 37^o to 180^o. During this motion, the CR is displaced by 3mm with respect to the initial one, see Fig. 5.

Based on the above mentioned conclusions a kinematical model for the lateral abduction of the human upper limb is presented briefly in the following section.

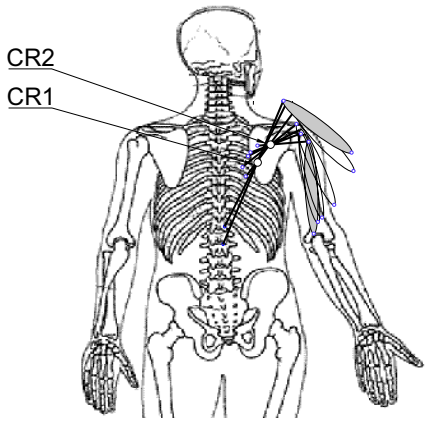

Fig.5. Locus of points obtained from the experiment and the two different instant CR of the humerous with respect to the scapula.

III. Kinematic Design and Analysis

An appropriate mechanism had to be designed that could reproduce the desired movement of the upper arm. The mechanism should be able to execute a complicated movement consisting of a rotational one about CR1 for 0^o to 37^o and a second rotational about CR2, 3 mm above CR1, from 37^o to 150^o. Furthermore, a mechanism for the transmission of torque to the first dof was needed. The proposed mechanism is described next.

Based on the experimental results, a mechanism that could produce an intermittent motion was searched and thus all the intermittent motion mechanisms were examined. Among the intermittent motion mechanisms, only the indexing mechanisms hold their position with a timed, unidirectional motion of the output member. For that reason a 4-sloted Geneva mechanism, [14], was used, as shown in Fig. 6. As shown in the same figure, the Geneva mechanism was used in conjunction to a four-bar mechanism, used for moving the arm CR, point C.

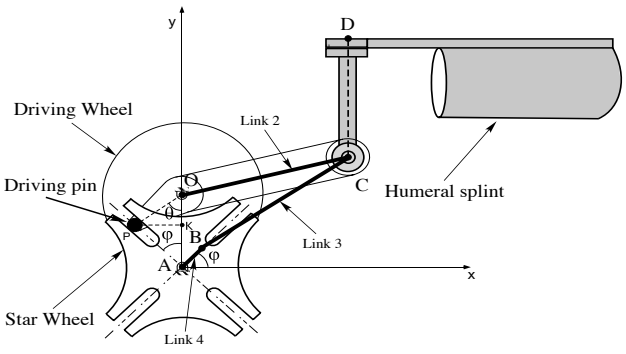

Fig. 6. Schematic representation of the 2-DOF mechanism with its kinematical parameters.

The driving wheel in Fig. 6 is rotated by a servomotor with $\theta°$ causing the intermittent motion of the star wheel. The wheel motion is described by the angle $\phi°$. Both angles are measured from the common centerline OA. The centerline of the slot must be tangent to the circle with radius $OP = r$, described by the center of the pin at the position in which the pin enters or leaves the slot. This condition dictates that the center distance of the two wheels OA must be $r\sqrt{2}$.

The expression $\phi = \phi(\theta)$ that relates the star wheel displacement to the displacement of the driving wheel can be found by solving the triangles $A\hat{P}K$ and $O\hat{P}K$ to obtain,

$$r\sin\theta = x\sin\phi \tag{1a}$$

$$r\cos\theta + x\cos\phi = r\sqrt{2} \tag{1b}$$

where r is the distance OP representing the radius of the pin circle and x the distance AP according to Fig. 6. By elimination of the term x from (1a) and (1b), the desired expression $\phi = \phi(\theta)$ is given by,

$$\phi = \tan^{-1}\left(\frac{\sin\theta}{\sqrt{2}-\cos\theta}\right) \tag{2}$$

The corresponding velocity of the star wheel, $\dot{\phi}$, is given by,

$$\dot{\phi} = \dot{\theta}\left(\frac{\sqrt{2}\cos\theta - 1}{3 - 2\sqrt{2}\cos\theta}\right) \tag{3}$$

and the corresponding acceleration by

$$\ddot{\phi} = \ddot{\theta}\frac{\sqrt{2}\sin\theta}{\left(3 - 2\sqrt{2}\cos\theta\right)^2} \tag{4}$$

with $-45° \le \phi \le 45°$ and $37° \le \theta \le 143°$. It must be mentioned that the Geneva mechanism is modified to work within the desired range. As the driving wheel rotates from 0^o to 37^o, the pin P slides into the slot resulting in a pure rotational motion of point C (center of rotation of the humerous) which is connected with point O by Link 2. As a result, the arm that lies inside the gray splint moves upwards, rotated about the instant center of rotation CR1. Therefore, until this point the mechanism produces an elevation of the arm from 0^o to 37^o.

After $\theta = 37°$, the instant CR starts moving upwards. In order to solve this problem the driving wheel's pin engages with the star wheel causing it to rotate. As the star wheel rotates point B rotates by $\phi°$ and when it comes to position B' it is clearly seen that the four-bar mechanism is moved causing point C to move upwards to $CR2$, see Fig. 7. The constant rotation of point C is secured by a transmission system consisting of two timing pulleys and a timing belt placed coaxial with points O and C. Their distance remains constant thanks to Link 2, providing thus constant rotation.

In order to obtain the kinematical equations of motion describing point C an analysis by loop closure equations is used. According to Fig. 8, the loop closure

equations for the four-bar mechanism created by OA (link 1) and links 2-4 are,

$$-r_2 \sin \vartheta_2 + r_3 \sin \vartheta_3 + r_4 \sin \vartheta_4 - r_1 = 0 \quad (5a)$$

$$r_2 \cos \vartheta_2 - r_3 \cos \vartheta_3 - r_4 \cos \vartheta_4 = 0 \quad (5b)$$

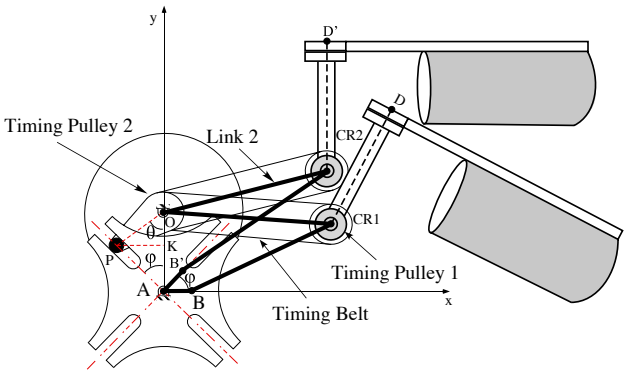

Fig. 7. Translation of the rotation center C representing the different CR in the human arm's elevation.

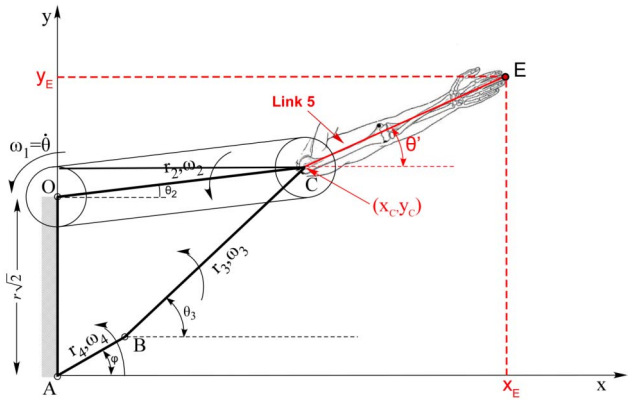

Fig. 8. Kinematic chain of the proposed mechanism for lateral abduction where C is the CR of humerous and E the end of arm.

Combining (5a-b), the following equation is obtained,

$$\begin{aligned} r_3^2 &= r_1^2 + r_2^2 + r_4^2 + 2r_1 r_4 \cos\phi - 2r_1 r_2 \cos\theta_2 \\ &\quad - 2r_2 r_4 \cos\phi \cos\theta_2 - 2r_2 r_4 \sin\phi \sin\theta_2 \end{aligned} \quad (6)$$

where the value of ϕ is given from (2) and the four link lengths r_1, r_2, r_3 and r_4 are known. Given these values, it is possible to solve (6) for the unknown θ_2. Using trigonometric identities and substituting them into (6), multiplying by $[\cos(\phi/2)]^{-2}$ and grouping terms gives

$$Kt^2 + Pt + Q = 0 \quad (7)$$

where

$$\begin{aligned} K &= r_3^2 - r_1^2 - r_2^2 - r_4^2 - 2r_1 r_4 \cos\phi - 2r_1 r_2 - 2r_2 r_4 \cos\phi \\ P &= 4r_2 r_4 \sin\phi \\ Q &= r_3^2 - r_1^2 - r_2^2 - r_4^2 - 2r_1 r_4 \cos\phi + 2r_1 r_2 + 2r_2 r_4 \cos\phi \\ t &= \tan(\theta_2/2) \end{aligned}$$

Knowing the expression for the unknown ϕ, the kinematical equations for point C and E are given by,

$$\begin{bmatrix} x_C \\ y_C \end{bmatrix} = \begin{bmatrix} r_2 \cos\theta_2 \\ r_1 + r_2 \sin\theta_2 \end{bmatrix} \quad (8)$$

and

$$\begin{bmatrix} x_E \\ y_E \end{bmatrix} = \begin{bmatrix} r_2 \cos\theta_2 + r_5 \cos\theta' \\ r_1 + r_2 \sin\theta_2 + r_5 \sin\theta' \end{bmatrix} \quad (9)$$

where

$$\theta' = \theta_2 + \theta \quad (10)$$

Differentiating (8) with respect to time, the velocity of the center C and the end of arm E is obtained from

$$\begin{bmatrix} \dot{x}_C \\ \dot{y}_C \end{bmatrix} = \begin{bmatrix} -r_2 \sin\theta_2 \\ r_2 \cos\theta_2 \end{bmatrix} \cdot \dot{\theta}_2 \quad (11)$$

$$\begin{bmatrix} \dot{x}_E \\ \dot{y}_E \end{bmatrix} = \begin{bmatrix} -r_2 \sin\theta_2 - r_5 \sin\theta' \\ r_2 \cos\theta_2 + r_5 \cos\theta' \end{bmatrix} \begin{bmatrix} \dot{\theta}_2 \\ \dot{\theta}' \end{bmatrix} \quad (12)$$

Differentiation of the velocity equations (11) and (12) with respect to time yields the acceleration equations

$$\begin{bmatrix} \ddot{x}_C \\ \ddot{y}_C \end{bmatrix} = \begin{bmatrix} -r_2 \cos\theta_2 \\ -r_2 \sin\theta_2 \end{bmatrix} \cdot \ddot{\theta}_2 \quad (13)$$

$$\begin{bmatrix} \ddot{x}_E \\ \ddot{y}_E \end{bmatrix} = \begin{bmatrix} -r_2 \cos\theta_2 & -r_2 \sin\theta_2 & r_5 \cos\theta' & -r_5 \sin\theta' \\ -r_2 \sin\theta_2 & r_2 \cos\theta_2 & -r_5 \sin\theta' & r_5 \cos\theta' \end{bmatrix} \begin{bmatrix} \dot{\theta}_2 \\ \ddot{\theta}_2 \\ \dot{\theta}' \\ \ddot{\theta}' \end{bmatrix} \quad (14)$$

Using velocity loop-closure equations and assuming that r_1, r_2, r_3, r_4 and ϕ are given, the expressions for angular velocity of links 2 and 4 are given by

$$\dot{\theta}_2 = \frac{FB - EC}{DB - AE} \quad (15)$$

$$\dot{\theta}_4 = \frac{DC - FA}{DB - AE} \quad (16)$$

where

$$\begin{aligned} A &= -r_2 \cos\theta_2 \\ B &= r_3 \cos\theta_3 \\ C &= -r_4 \cos\theta_4 \cdot \dot{\theta}_4 \\ D &= -r_2 \sin\theta_2 \\ E &= r_3 \sin\theta_3 \\ F &= -r_4 \sin\theta_4 \cdot \dot{\theta}_4 \end{aligned} \quad (17)$$

Following the identical procedure and acceleration loop-closure equations and assuming that the values of $r_1, r_2, r_3, r_4, \theta_2, \dot{\theta}_2, \theta_3$ and $\dot{\theta}_3$, are known from velocity analysis, the expressions for angular acceleration of links 2 and 4 are given by

$$\ddot{\phi}_2 = \frac{F'B - EC'}{DB - AE} \quad (18)$$

$$\ddot{\phi}_4 = \frac{DC' - F'A}{DB - AE} \tag{19}$$

where

$$\begin{aligned} A &= -r_2 \cos\theta_2 \\ B &= r_3 \cos\theta_3 \\ C' &= -r_2\dot{\theta}_2^2 \sin\theta_2 + r_3\dot{\theta}_3^2 \sin\theta_3 + r_4\dot{\theta}_2^2 \sin\theta_4 - r_4\ddot{\theta}_4 \cos\theta_4 \\ D &= -r_2 \sin\theta_2 \\ E &= r_3 \sin\theta_3 \\ F' &= r_2\dot{\theta}_2^2 \cos\theta_2 + r_3\dot{\theta}_3^2 \cos\theta_3 - r_4\dot{\theta}_2^2 \cos\theta_4 - r_4\ddot{\theta}_4 \sin\theta_4 \end{aligned} \tag{20}$$

Fig. 9 shows plots of (2), (3) and (4) for $-45° \le \phi \le 45°$.

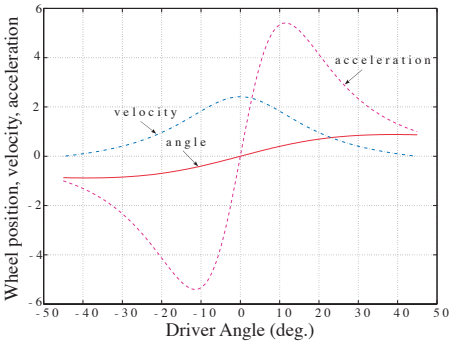

Fig. 9. Position, velocity and acceleration of the driven wheel of the Geneva mechanism with 4-slots.

The output torque of the star wheel is given with respect to the servomotor input torque as,

$$\frac{T_{out}}{T_{in}} = \left(\sqrt{2}\cos\theta - 1\right) \tag{18}$$

where T_{out} is the output torque of the star wheel and T_{in} the engine torque applied. The torque transmission ratio in (18) is displayed in Fig. 11.

Based on the kinematical equations described, an estimation for the required motor torque was made and a motor was chosen. The nature of the required torque for the abduction and adduction of the human arm is seen in Fig 10, noting that the maximum torque is about 2Nm.

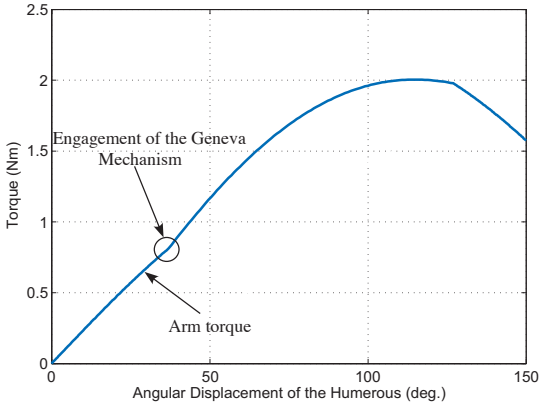

Fig. 10. Motor torque as a function of humerous angular displacement.

Eq. (19) gives the frictional force experienced by the slot as it engages with each slot,

$$\frac{F_{slot}}{F_c} = \mu\left(\frac{\sqrt{2}\sin\theta}{\sqrt{3 - 2\sqrt{2}\cos\theta}}\right) \tag{19}$$

where μ is the coefficient of kinetic friction and F_c the constant force applied by the pin on the slotted wheel. Eq. (19) is plotted in Fig. 11.

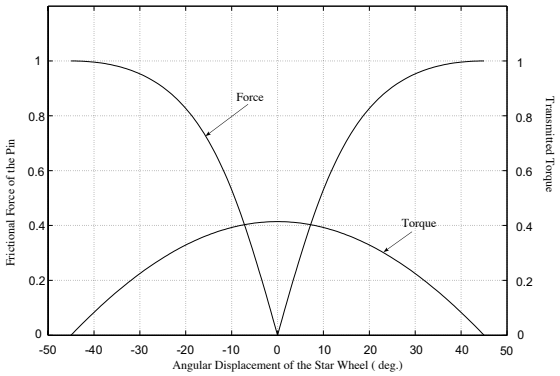

Fig. 11. Transmitted torque and frictional force as a function of angle of rotation θ.

IV. Design Validation

The effectiveness of the proposed design for the lateral abduction was tested using Lego elements, see Fig. 12. As far as the frontal abduction is concerned, there were no major problems encountered apart from mechanism singularities. These were moved in order not to interfere with a smooth arm elevation.

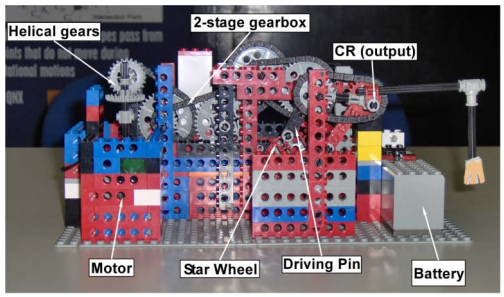

Fig. 12. Lego model of the proposed mechanism for the lateral abduction of human right arm.

The Lego model constructed consists of a motor with an incorporated gear head, see Fig. 12. The output of the motor changes direction by 90° through a couple of helical gears and then driven through a two-stage gearbox to the Geneva driven wheel. The driving pin engages with the slot of the star wheel, causing the CR to move upwards, yielding the lateral abduction of the (right) arm.

Next, a 3D CAD model was designed in order to examine its strength and make a primarily selection of the material to be used. Therefore, both a static and modal analysis was made. Quite a few materials were tested, among them

epoxy, *kevlar*, *PVC*, *medical steel* and a low-alloy *steel.* The 3D CAD model was imported into a FEA package and the results showed that the best material was epoxy resins, see Fig. 13. Four natural frequencies were obtained from modal analysis in the range of 5 to 30 Hz.

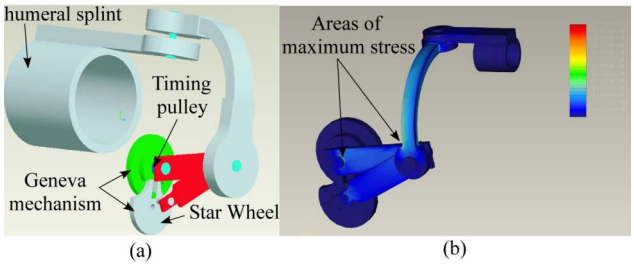

Fig. 13. (a) 3-D CAD model of the proposed 2-DOF mechanism for the frontal and lateral abduction, (b) FEA mechanism verification.

The design of the mechanism's components was carried out with the target of minimizing the total weight keeping the required stiffness of it. The values of some critical dimensions, based on the sensitivity analysis made, were changed according to an optimization technique used along with FEA. In particular, the length and diameter of cantilever mounted on the star wheel of the Geneva mechanism was optimized yielding the best results for minimum weight and appropriate strength. The optimization results are illustrated in Fig. 15. The total weight of the proposed mechanism was estimated about 1.6 kg and the maximum stress about 230 N/mm^2 with the maximum displacement at 2.7 mm.

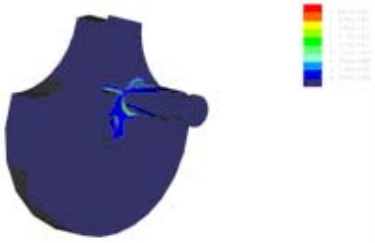

Fig. 14. Optimization on both length and diameter of the cantilever mounted on the star wheel of the Geneva mechanism.

V. Conclusions

In this paper, we were interested in developing an exoskeleton mechanism for the human upper arm. A brief analysis of the existing exoskeletons showed that these were either unactuated or not portable while almost none of them considered the translational motion of the CR of the humerous with respect to the scapula. An experimental procedure was used in order to determine the kinematics of the lateral and frontal abduction using a CMM machine and a plastic humeral splint. The experimental results revealed the complex motion of the area, yielding the position of the two CRs. Based on these results, a novel hybrid mechanism for the lateral abduction was proposed, based on a combination of a Geneva and a four bar mechanism. The validation of the mechanism done using Lego elements and a CAD package illustrated its effectiveness, showing that it can reproduce the desired type of movement, i.e. lateral and frontal abduction of the human upper arm.

References

[1] E. J. McCormick, Ed., *Human Factors Engineering, 3rd ed.* New York: McGraw-Hill, 1970.

[2] D.W. Repperger, S. J. Remis, and G. Merrill, "Performance measures of teleoperation using an exoskeleton device," in Proc. *of the IEEE Intl. Conf. on Robotics and Automation,* Cincinnati, May 1990, pp. 552-557

[3] G. R. Johnson, D. A. Carus, G. Parrini, S. S. Marchese, and R. Valeggi, "The design of a five-degree-of-freedom powered orthosis for the upper limb," in *Proc. Instn. Mech. Engrs. Part H,* vol 215, 2001, pp. 275-284.

[4] M. A. Buckley and R. R. Johnson, "Computer simulation of the dynamics of a human arm and orthosis linkage mechanism," in *Proc. Instn. Mech. Engrs. Part H,* vol 211, 1997, pp. 349-357.

[5] Kazuo Kiguchi, Toshio Fukuda : "A 3DOF Exoskeleton for Upper-Limb Motion Assist –Consideration of the Effect of Bi-Articular Muscles", *Proceedings of IEEE International Conference on Robotics and Automation (ICRA'04)*, New Orleans, LA, pp.2424-2429, 2004.

[6] Kazuo Kiguchi, Koya Iwami, Makoto Yasuda, Keigo Watanabe, Toshio Fukuda : "An Exoskeletal Robot for Human Shoulder Joint Motion Assist", *IEEE/ASME Trans. on Mechatronics*, vol.8, no.1,pp.125-135, March, 2003.

[7] Kazuo Kiguchi, Takakazu Tanaka, Keigo Watanabe, Toshio Fukuda : "Design and Control of an Exoskeleton System for Human Upper-Limb Motion Assist*", Proceedings of 2003 IEEE/ASME International Conference on Advanced Intelligent Mechatronics (AIM 2003)*, pp.926-931, Kobe, 2003.

[8] Kazuo Kiguchi, Koya Iwami, Keigo Watanabe, Toshio Fukuda : "A Shoulder Joint Motion Support System for Rehabilitation", *Proc. of the 11th International Conference on Advanced Robotics (ICAR'03)*, vol.1, Portugal, June 30-July 4, 2003, pp.11-16.

[9] Kazuo Kiguchi, Takakazu Tanaka, Keigo Watanabe, Toshio Fukuda : "Exoskeleton for Human Upper-Limb Motion Support", *Proceedings of IEEE International Conference on Robotics and Automation (ICRA'03)*, Taipei, 2003, pp.2206-2211.

[10] Kazuo Kiguchi, Makoto Yasuda, Koya Iwami, Keigo Watanabe, Toshio Fukuda : "Design of an Exoskeletal Robot for Human Shoulder Motion Support Considering a Center of Rotation of the Shoulder Joint", *Proceedings of IEEE/RSJ International Conference on Intelligent Robots and Systems (IROS'02)*, 2002, pp.1493-1498.

[11] Kazuo Kiguchi, et al., "Intelligent Interface of an Exoskeletal Robot for Human Elbow Motion Support Considering Subject's Arm Posture", *Proc. IEEE International Conference on Fuzzy Systems (FUZZ-IEEE 2002) (WCCI 2002)*, 2002, pp.1532-1537.

[12] Kazuo Kiguchi, et al., "A Study of an Exoskeletal Robot for Human Shoulder Motion Support", *Proceedings of IEEE/RSJ International Conference on Intelligent Robots and Systems (IROS'01)*, 2001, pp. 2111-2116.

[13] Wu Ge, et al., "ISB recommendation of definitions of joint coordinate systems of various joints for the reporting of human joint motion-Part II: shoulder, elbow, wrist and hand," *Journal of Biomechanics*, Vol. 35, No. 4, pp. 543-548.

[14] Mabie Hamilton H., Charles F. Reinholtz, *Mechanisms and Dynamics of Machinery*, 4th edition, Wiley, 1987.

[15] FARO Technologies, Inc., *FARO Arm Users Manual*, www.faro.com.

[16] NK. Poppen, PS. Walker, "Normal and abnormal motion of the shoulder", *The Journal of Bone and Joint Surgery*, Vol. 58, Issue 2, pp. 195-201, 1976.